MEDWIN PUBLISHERS
Committed to Create Value for Researchers

Petroleum & Petrochemical Engineering Journal
ISSN: 2578-4846

# Mobility Control Potential in Geological Sequestration of Anthropogenic Carbon Dioxide using Cheap Soluble Organics as Thickeners and Implications for Interfacial Stability

**Miadonye A* and Amadu M**

School of Science and Technology, Cape Breton University, Canada

***Corresponding author:** Miadonye A, School of Science and Technology, Cape Breton University, Nova Scotia, Canada; Email: adango_miadonye@cbu.ca

**Review Article**

**Volume 5 Issue 4**

**Received Date:** December 07, 2021

**Published Date:** December 31, 2021

DOI: 10.23880/ppej-16000290

## Abstract

Current levels of anthropogenic carbon dioxide in the atmosphere are responsible for global warming at scales not seen before. To mitigate this global warming trend, the Intergovernmental Panel on Climate Change (IPCC) has universally adopted the geological carbon storage option. The technical implication of geological carbon storage is that carbon dioxide with a very low dynamic viscosity will be injected to push formation brine with a high viscosity contrast. Consequently, problems of interfacial instability responsible for poor sweep efficiencies encountered in the petroleum industry's improved oil recovery projects are inevitable. The petroleum industry has used costly mobility control agents in the form of carbon dioxide thickeners to solve problems of poor sweep efficiency in carbon dioxide enhance oil recovery projects. This experience is useful to the geological sequestration community because carbon dioxide geological storage under supercritical conditions is considered an optimized approach. In this paper, We have reviewed literature to show the solubility of waste organics in supercritical carbon dioxide and the possibility to increase its dynamic viscosity to reduce interfacial instability problems. We have, also, reviewed literature to show sources and availability of cheap soluble organics for carbon dioxide thickening. Our review shows promising sources of these soluble organics. Finally, the technical implications of dynamic viscosity increase on a given geological storage project have been discussed in the context of interfacial stability theories.

**Keywords:** Viscosity; Supercritical; Mobility control; Carbon dioxide thickeners; Sweep efficiency; Stability

## Introduction

Global warming and the attendant climate change [1] due to anthropogenic sources of greenhouse gases – ($CO_2$) and oxides of Nitrogen ($NO_x$) from combustion sources is the major environmental problem of the twenty-first century [2]. This environmental issue has prompted the evolution of socioeconomic agenda at all levels of economic and technological development to deal with economic and social dimensions of the phenomenon [3]. The huge increase in demand for energy in the wake of the industrial revolution and the periods after coupled with the relatively low technology available for hydrocarbon fluid exploration and production led to unprecedented combustion of coal to meet the energy needs of society. This caused exponential growth trends [4]. The immediate effect of the exponential release of $CO_2$ and other greenhouse gases into the atmosphere was not seen until the latter part of the twentieth century.

In the context of the global carbon budget which reflects the balance between anthropogenic emissions and the dynamics of sinks which removes them, anthropogenic carbon growth rate is governed by two principal factors or carbon fluxes [5]. They are carbon emissions fluxes from

fossil fuel combustion and industrial processes and the fluxes from land use practices which are further governed by socioeconomic factors. Accordingly, recent trends in anthropogenic carbon emission data show that emission is strongest in developed and rapidly developing economies of the world. These economies together accounting for 80% of global population were directly responsible for 73% of global emissions in 2004 while in the mid-18$^{th}$ Century they only accounted for only 41%. These represent definite accelerating trends in fossil fuel combustion with the growth increasing from nearly 1.1% between 1990 and 1999 to over 3% between 2000 and 2004 [6]. These concerns led to the international Convention on climate change and global warming held in Kyoto [7] and Copenhagen [8]. Furthermore, radiative forcing due to the well-mixed greenhouse gases indicates that $CO_2$ accounts for 64% of the total radiative effect [9].

To curb global warming due to greenhouse gas release requires not only reducing emissions but also reducing the level of greenhouse gas present in the atmosphere. The global consensus about emission reduction is to isolate greenhouse gases, notably $CO_2$, which accounts for the major composition of flue gas from fossil fuel combustion [10]. The isolation of $CO_2$ can be carried out in several potential locations; namely deep unmineable coal seams, depleted oil and gas reservoir, salts caverns, and deep saline aquifers [11]. In addition to these geologic repositories, sequestration in deep oceans is also a possibility [12]. Accordingly, judging from experience gained by the petroleum and environmental industries about fluid injection into hydrocarbon reservoirs for improved oil and gas recoveries and for disposal of waste waters into geologic repositories respectively, such operations involve two-phase flow of immiscible fluids in porous media. The efficiency at which this task can be accomplished for a given project depends very much on the stability of the two-phase flow hydrodynamics. In this regard, a well-documented instability problem known in the petroleum industry is viscous fingering which occurs when an injected fluid of low dynamic viscosity is made to displace a resident fluid of higher viscosity resulting in an unfavorable viscosity contrast [13].

Viscosity modifiers that can increase the viscosity of injected fluids have been used in the petroleum industry to solve the viscous fingering instability problem. These are costly mobility control agents. In view of geological sequestration being an added cost to the power industry, a cheaper mobility control agent must be sought. Considering the recommended supercritical sate for $CO_2$ sequestration to ensure maximization of available pore space, certain organic solutes that are by-products from other industries as well as waste grease from households can be made to dissolve in supercritical carbon dioxide because of the enhanced solvent ability supercritical state fluids [14].

This work has three principal objectives. The first is to make the carbon geosequestration community aware of abundant resources as potential mobility control agents that are either cheap or are by-products [15] of certain industries and can be taken free of charge or without significant cost. The second is to create awareness in the geosequestration community of the potential for sustainable availability of these cheap potential mobility control agents in the light of current and anticipated future technological advances in those industries that produce them [16]. The third is to discuss the effect of viscosity increase on geological storage of anthropogenic carbon dioxide in the context of existing theories on interfacial stability.

## Dynamic Viscosity of Supercritical Carbon Dioxide and Brine under Geological Sequestration Condition

One characteristic of SC-$CO_2$ injection for geological storage is the extent of plume evolution. Generally, the extent of plume evolution is period dependent such that during the injection period plume evolution will depend on the relative strength of gravity to viscous forces. During the post injection period, the dominant forces are gravitational, and this favors dominant plume evolution. To predict plume evolution, Nordbotten, et al. [17], specified the dynamic viscosity of supercritical carbon dioxide and brine based on basin classification into colder and warmer ones. In this regard, basins with geothermal gradient of 25 $^{o}$C/km are referred to as colder basins while those with a geothermal gradient of 45$^{o}$C/km are warmer ones. Table 1 shows values of phase viscosities.

| | | Colder basin (mPa.s) | Warmer basin (mPa.s) |
|---|---|---|---|
| Shallow formation | gas | 0.0577 | 0.0233 |
| | brine | 0.795-1.58 | 0.491-0.883 |
| Deep formation | gas | 0.0611 | 0.0395 |
| | brine | 0.378-0.644 | 0.195-0.312 |

**Table 1:** Dynamic viscosity of Supercritical Carbon Dioxide and Brine for Colder and Warmer Basins [17].

Figure 1 below from Preuss and Garcia [18] shows a generalized chart of carbon dioxide viscosity as function of temperature and pressure. The figure shows that at typical geologic conditions of carbon dioxide sequestration (31°C, 73.7) and above, the dynamic viscosity is far lower than that of formation brine.

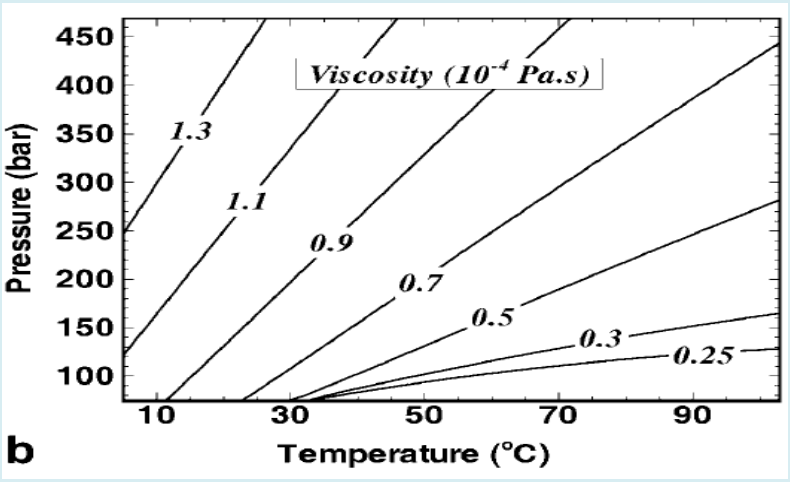


**Figure 1:** Dynamic viscosity of carbon dioxide as a function of temperature and pressure [18].

## Hydrodynamic Instabilities during $CO_2$ Injection

### Convective and Viscous Fingering Instabilities

In addition to the geomechanical effect related to cap rock mechanical loading during $CO_2$ injection into geologic media, significant difference between injected $CO_2$ and resident brine viscosity constitutes a major hydrodynamic instability problem related to viscous fingering [19]. Campbell and Orr [20] studied Flow visualization for $CO_2$/crude-oil displacements in a porous system. They noted two principal causes of interfacial instability. They are heterogeneities and adverse viscosity ratio. For a homogeneous system with nearly the same pore size distribution, the flood advance was uniform as opposed to a system with heterogeneity. When the viscosity ratio of oil-to carbon dioxide was 22, the front was characterized by viscous fingers compared to a sharp front where the ratio is 50.

The other type of instability is convective instability that becomes manifest during the post injection periods [21]. One fundamental dimensionless parameter that governs displacement during $CO_2$ injection into a saline aquifer is the gravity number defined as the ratio of viscous forces to gravity forces. During the injection period, viscous forces dominate the hydrodynamics of the system resulting in a gravity number greater than unity. In the post injection periods, gravity forces dominate and this causes the gravity override effect where buoyant $CO_2$ migrates upward and by encountering fresh brine at higher depths, corresponding to low temperature-salinity environments dissolves to produce brine of higher densities. These high-density brines sink causing fresh brine to be made available to ascending $CO_2$ gas. This type of instability is an essential requirement for carbon sequestration by solubility trapping, which is expected to lead to ultimate safe and permanent carbon geosequestration by geochemical reactions. This will lead to stable carbonates after hundreds or thousands of years [22]. Compared to convective instability, viscous fingering hydrodynamic instability is an unfavorable condition that has the obvious potential to compromise both fluid injection efficiency and geostorage capacity and, therefore, deserves attention. To mitigate the effect requires increasing the viscosity of the injected gas phase with the prime aim of increasing the sweep efficiency of the displacement by enhancing favorable viscosity ratio [23]. This is mobility control because the viscosification of the injected gas reduces its phase mobility.

### Effect of Low Viscosity Ratio on Geological Sequestration Capacity

A gross reduction on the storage capacity of a geologic repository is to be expected because of low viscosity ratio. For example, van Engelenberg and Block [24] contended that a reduction of about an order-of-magnitude of the sequestration capacity of aquifers in the Netherlands can occur if the low viscosity of carbon dioxide is taken into consideration in capacity estimates. This means if the dynamic viscosity of carbon dioxide could be increased, this trend in reduction can be reversed [20].

## Viscosification of Carbon Dioxide

### $CO_2$ Thickeners in the Petroleum Industry

Experience from hydrocarbon field development shows that out of the original oil in place only a third can be produced using conventional depletion drive mechanisms which rely on rock and fluid expansion to cause flow of hydrocarbon fluids to production wells. The remaining oil in place can be produced using conventional secondary recovery by water injection. To optimize resource recovery, production of additional oil from the reservoir at residual oil saturation is possible using tertiary oil recovery, such as $CO_2$ flooding [25]. This technology can pressurize the reservoir as well as reduce the dynamic viscosity of oil by dissolution. However, in view of the sharp contrast between injected $CO_2$ and resident oil viscosity the efficiency of the flooding can only be improved by increasing the viscosity of the injected gas. The United States Department of Energy has estimated that if the viscosity of $CO_2$ could be tripled or quadrupled, domestic oil production rates could increase from 180,000 barrels per day to 400,000 barrels per day [26]. Consequently, the petroleum industry has used $CO_2$ thickeners to achieve this goal. Some of these thickeners have been in the form of trialkytin fluorides [27], and low molecular weight telechelic ionomers that are considered suitable [28].

Apart from these compounds, polymers having higher molecular weights that have the capability to increase solubility mostly by chain enlargement were also used as thickeners in the petroleum industry [29]. However, due to the very low solubility of these thickeners in $CO_2$ it is obvious that their solubility in the dense phase gas is even far lower unless the use of co-solvents can be promoted. Under normal reservoir conditions $CO_2$ is generally found in the super critical state (SC-$CO_2$). Consequently, to meet the ultimate objective of tertiary oil recovery by $CO_2$ flooding, highly soluble molecular weight thickeners have evolved in the petroleum industry in the form of $CO_2$-philic functional groups consisting of fluoroacrylates, fluoroethers, fluoroethanes and silicones [30]. The $CO_2$-philic functional groups and nonfunctional groups mentioned earlier have solubility characteristics determined by temperature, pressure and co-solvent proportions and the most significant aspect of their utilization in tertiary oil recovery must do with cost analysis. Another most promising $CO_2$ thickener has been identified [31]. This polymer has a number average molecular weight of 540,000 with a polydispersivity index of 1.63 with high solubility in dense $CO_2$.

### Cost Overview of $CO_2$ Thickening

Copolymers used in traditional carbon dioxide viscosification are very expensive. For instance, the lowest price of fluoroacrylate polymers is on the order of 50 USD-per 1001 lb [32]. Enick, et al. [32] identified an environmentally friendly carbon dioxide-thickener that is two orders of magnitude less expensive that the fluoroacrylate-styrene copolymer. Consequently, an inexpensive $CO_2$-thickener that can increase the mobility ratio would enhance the sequestration capacity of aquifers and oilfields.

## Sources of Soluble Organics for Carbon Sequestration

### Concept

In this paper, we consider soluble organics as those organic materials derived from animal and plant sources that exhibit various degrees of solubility in SC-$CO_2$ and are cheaper to use for viscosification and mobility control purposes. These are invariably, fats from animal and plant sources that mostly constitute by-products from domestic and commercial activities of the agrosectors of the economy.

### Soluble Organics from Slaughterhouses

Fats are important sources of slaughterhouse waste/by-products that can be of economic value in a number of respects. In Belgium, approximately 20 companies collect animal fats from slaughterhouses and render this into homogeneous substances that are sold to animal feed producers [33]. In cattle alone, 39% of the live weight comprises organs, fat tissue, bone and blood [34]. Apart from by-products from the slaughterhouses, the fish industry is also a significant source of waste soluble organics in the form of fats. Also, waste products from fish processes are known to contain 19% percent fatty components. Elsewhere [35], waste products from fish processes is known to contain 19% percent fatty components.

### Shea Butter

The shea butter tree (Vitellaria paradoxa) is found solely in Africa's Sudano-Sahelian region where it thrives with just 500–1,000 mm of rainfall [36]. It is generally long lived and can attain an age of 200–300 years with a slow characteristic growth. The tree begins fruiting after five years and attains full fruiting capacity after fort–fifty years [37]. The fruiting begins during the month of May and continues until the late September. An adult tree produces an average of 20 kg of fresh fruit annually and a corresponding 4 kg of dried nut and between 0.7 to 2.5 kg of butter annually, this amount of butter being dependent on the extraction method. The global demand for Shea butter has stimulated production and exportation throughout the Africa Sahel region. Burkina Faso is the region's leading Shea butter production and exporter accounting for about 25% of global annual export. Medieval

Arabic and European sources document the prevalence of Shea butter in the market and households throughout the West African savannah and Sahel regions [38]. Export for Shea nut and shear butter continue to grow. Between 1995 and 1997 exports from Ghana leaped from 15,000 tonnes to 32,000 tonnes and this constitutes an increase in annual revenue from two to seven million dollars United States Dollars. For Burkina Faso, the export increased from 9,964 tons to 34975 tons over the period lasting from 1997 to 2002 as shown in Table 2.

| Year | Shea nuts (tons) |
|---|---|
| 1997 | 9,964 |
| 2000 | 11,575 |
| 2001 | 17,980 |
| 2002 | 34,975 |

**Table 2:** Shear Export from Burkina Faso for Selected Years (1997-2004) [39].

## Soluble Organics from Waste Cooking Oil

Waste cooking oil is defined as oils generated during cooking from the use of fresh cooking oils or from sources of proteins of animals and plant origin. Generally, the physical and chemical properties of waste cooking oil are almost like those of fresh edible oils and vary from one source of waste cooking oil to the other. The water content is generally higher than that of fresh cooking oil with dynamic viscosity, heat capacity and surface tension being higher. These changes result from normal cooking processes such as frying which can induce oxidative, hydrolytic and thermolytic reactions [40]. Waste cooking oil is generated after routine cooking in restaurants and household kitchens and can be a mixture of fats from different sources *viz* animal and vegetable proteins. In China, environmental authorities take large quantities of waste cooking oils from restaurants for safe disposal in accordance with environmental regulations [40]. The annual amount of waste cooking oil generated as waste grease in each country depends on the use of vegetable oil. A 1998 report Wiltsee G [41], showed that ~ 4kg of yellow grease per person was produced annually in the United States. With the increase in population this amount has likely increased proportionally.

The desire to consider waste cooking oil as a potential feed stock for biodiesel production through the process of transesterification has led to studies that have revealed a huge potential of waste cooking oil generation worldwide [42]. In the European Union alone the total waste cooking oil production was estimated to be approximately 700,000 – 1,000,000 tonnes/yr [40]. Cost wise waste cooking oil is much cheaper compared to fresh cooking oils with yellow grease, a waste cooking oil from soya bean oil being 1.09 USD per gallon with a possibility price rise to 1.21 USD per gallon.

Table 3 sums up trends in waste cooking oil generation for selected countries. The statistics revealed by this table testifies to the potential for sustainable use of waste cooking oil not only for biodiesel but also for $CO_2$ viscosification.

| Country | Quantity $10^6$ tonnes/y) | Source of oil |
|---|---|---|
| Canada | 0.12 | Animal fat, canola oil |
| China | 4.5 | Salad oil, animal fat |
| Japan | 0.45–0.57 | Soybean oil, palm oil, animal fat |
| Malaysia | 0.5 | Palm oil |
| Taiwan | 0.07 | Soybean oil, palm oil, beef oil, lard oil |
| United States | 10 | Soybean oil |

**Table 3:** Waste cooking oil generation from selected countries after [43].

In addition, large quantities of water cooking oils and animal fats are available worldwide, much of this coming from developing countries. Due to disposal problems, their availabilities in such huge volumes pose environmental and waste management challenges. In the United States, alone the *per capita wastes* cooking oil is 9 pounds and this amounts to an estimated 100 million gallons per day [44]. Per Statistics Canada, the total population is 33 million. Total produced waste cooking oil could be 135,000 tons/year [45]. The European Union contribution to waste cooking oil production by the advanced countries is reported to be approximately 700,000-1000000 tons/year [40], with the United Kingdom producing over 200,000 tons per year [46]. In some places, large amounts of waste cooking oils are illegally dumped into water bodies and landfills which come with environmental degradations.

## Solubility in Supercritical Carbon Dioxide (SC–$CO_2$)

The great potential of SC-$CO_2$ as an extraction solvent is well established in the food and pharmaceutical industries. This potential coupled with its readily accessible super critical state and nontoxicity has prompted a number several studies in these industries designed to explore commercial scale applicability [47]. In this study, cholesterol extraction from egg using supercritical carbon dioxide at varying temperatures and pressures was found to be encouraging. In addition, SC-$CO_2$ has been used for extracting and fractionating essential oils that deteriorate at higher temperatures from sources of vegetables [48]. The solubilities of organics in SC-$CO_2$ suggested by the present paper as potential for mobility control agents stems from the observation that vegetables are important and abundant sources of these organics [49]. While much of the solubility data for these organics abounds in the scientific community it is only known to the industries concerned and for that matter useful to chemical engineers and the pharmacists. It is, therefore, appropriate in this paper to endeavor to give an overview of their solubility potential in SC-$CO_2$ for the benefit of the carbon geosequestration community. The solubility of animal fats in SC-$CO_2$ has already been documented about the extraction of fat from pig skin animal skins [50]. In the leather industry, increased solubility of animal fat in SC-$CO_2$ has been exploited for producing high grade leather product [51]. Consequently, in view of the promising availability of waste cooking oil, coupled with its cheaper prices, the solubility of these organics in addition to fats from animal and plant sources constitute a potential for mobility control agents for carbon geosequestration projects. Table 4 shows the extractability of fats with SC-$CO_2$. The residual fat reported in Table 3 was determined by extraction with methylene chloride after the degreasing process. The data reported in Table 4 are the mean and standard deviations taken from the replicate runs presented in Marsal, et al. [51].

| $CO_2$ density (g/ml) | Extracted fat[01] (mg) | Residual fat[b] [02](mg) | Total fat (mg) | Degreasing efficiency (%) |
|---|---|---|---|---|
| 0.55 (104 bar) | 2.38 ± 1.18 | 39.90 ± 3.89 | 42.50 ± 3.02 | 5.70 ± 2.99 |
| 0.70 (133 bar) | 7.88 ± 3.92 | 34.95 ± 4.84 | 42.83 ± 4.39 | 18.33 ± 8.29 |
| 0.85 (240 bar) | 23.58 ± 0.87 | 20.20 ± 1.63 | 43.78 ± 1.11 | 53.88 ± 2.78 |

**Table 4:** Extractability in SC-$CO_2$ [51].
[01]Fat extracted by supe$_{rc}$ritical CO2
[02]Fat determined by extraction with chloride after the degreasing process

## Solubility of Waste Cooking Oil

Waste cooking oil is the product of used cooking oils which are lipids containing high proportions of triglyceride, an ester derivative of glycerol and fatty acid [52]. Generally, they are fats that have both polar and nonpolar parts, but the extensive chain of carbon hydrogen bonds renders them generally non-polar. It is, therefore, expected that since likes dissolve likes triglycerides will dissolve in carbon dioxide or in its super critical form and this forms the basis for supercritical carbon dioxide extraction of the lipids or fresh cooking oil. To determine whether waste cooking oil derived from fresh cooking oil in the process of cooking will have an appreciable solubility required to viscosify supercritical carbon dioxide it is appropriate to understand the various chemical reactions and transformation of the oil in the cooking process. Generally, three types of chemical reactions are distinguished in the process of cooking. Thermolytic reactions occur at temperatures in the range of 180°C in the absence of oxygen and result in the production series of normal hydrocarbons (alkanes, alkenes) lower fatty acids, symmetric ketones, oxypropyl esters, carbon monoxide and carbon dioxide. Subsequent reactions result in the formation of dimmers. Oxidative reactions occur in the presence of oxygen and this involves unsaturated fatty acids via free radical chain reactions with products being hydrocarbons, aldehydes, semi aldehydes and acids. Hydrolytic reactions result from the interaction of steam derived from food and the cooking oil leading to the formation of free fatty acids, glycerol, mono and diglycerides. Generally, the change in fresh cooking oil composition during the hydrolytic reaction is measured by quantifying the monoglyceride and diglyceride content of the oil after the cooking process. Figure 2 shows the intensities of triglyceride (TG), monoglycerides (MG) and diglycerides (DG) of fresh palm oil while Figure 3 shows similar compositions for treated waste cooking oil for different time of extraction, which includes high molecular weight components (HMWC). Table 5 compares the composition of fresh cooking oil, which includes Low molecular weight components (LMWC), used cooking oil and treated waste cooking oil compositions while Table 6 gives the composition and properties of fresh palm oil (FPO), heat treated palm oil (HTPO), fresh soybean oil (FSO) and waste soybean oil (WSO).

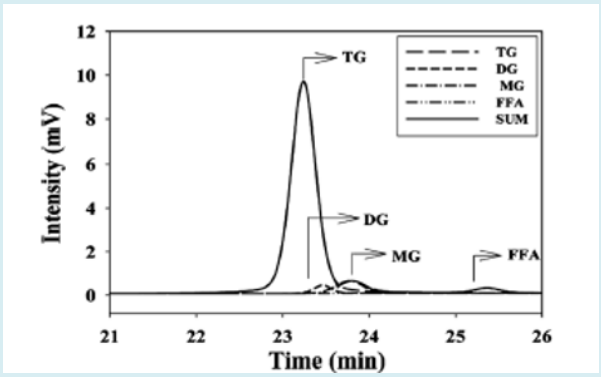


**Figure 2:** Intensities of components in waste cooking oil [53].

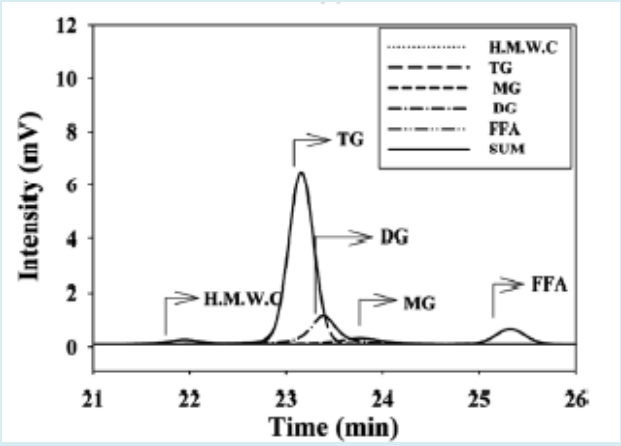


**Figure 3:** Intensities of components in waste cooking oil [53].

| Liquid fraction (%) | Fresh frying oil | Used frying oil | One stage treated oil[3] | Two stage treated oil[4] |
|---|---|---|---|---|
| TG | 92.7 | 70.1 | | |
| Polar | 7.3 | 29.9 | 15.1 | 9.1 |
| MMWC | 3.4 | 13.0 | 2.5 | 1.6 |
| LMWC | 3.9 | 16.9 | 12.6 | 7.5 |

**Table 5:** Comparison of the composition of fresh cooking oil, waste cooking oil and treated cooking oil [54].
[3]P = 300 kg/cm2, T= 40 oC, cosolvent type = hexane, cosolvent concentration = 10%.
[4]Composition of the fraction obtained after 4 h of extraction.

| Sample | HMWC (%) | TG (%) | DG (%) | MG | FFA | Acid value | CD | TPC |
|---|---|---|---|---|---|---|---|---|
| FPO | 0 | 91.2 | 2.5 | 5.6 | 0.7 | 0.22 | 0.077 | 9.19 |
| HTPO | 4.6 | 70.1 | 16.2 | 6.8 | 2.4 | 0.49 | 0.114 | 22.8 |
| FSO | 0.3 | 97.9 | 0.45 | 0.55 | 0.8 | 0.12 | 0.098 | 10.4 |
| WSO | 4.4 | 77.7 | 9.88 | 6 | 2 | 0.52 | 0.193 | 26.1 |

**Table 6:** Composition and properties of fresh palm oil, heat-treated soybean oil, and waste soybean oil [53].

Generally, the mono and diglycerides are polar in nature and their production during the hydrolytic reactions result in an increase in the composition of the polar fraction of cooking oils as seen in Tables 4 and 5.

### Viscosity of SC–$CO_2$ Containing Organic Solutes

Supercritical carbon dioxide has a liquid like behavior in view of its high density and a gas like behavior in view of its viscosity being in the ranges of the viscosity of gaseous materials. This unique physical property coupled with the fact that its critical point is comparatively lower than other potential solvents; it is used extensively in supercritical fluid extraction. To obtain an idea about the potential for supercritical carbon dioxide thickening using dissolved organics this paper will exploit already existing published works relating to super critical carbon dioxide viscosity measurements where different organic solutes have been used.

The viscosities of supercritical carbon dioxide (SC-$CO_2$) containing different levels of methyl oleate and oleic acid were measured with a high-pressure capillary viscometer. The SC-$CO_2$ -methyl-oleate system was evaluated at 313.15, 323.15 and 333.15 K and 11.5, 13.7 and 15.5 MPa, respectively. The SC-$CO_2$ -oleic acid system was evaluated at 313.15 K and 20.5 and 30.0 MPa and 333.15 K and 30.0 MPa. The increase in SC-$CO_2$ viscosity was as high as 15-20% at the maximum methyl-oleate concentrations (4-5 wt%) and 6-12% at the maximum oleic acid concentrations (2-3 wt%). The increase of relative viscosity with concentration was linear. Tables 7 & 8 indicate viscosity increases of SC-$CO_2$ containing oleic acid.

| T= 313.15 K; P =5 MPs<br>SC-$CO_2$ viscosity = 5.610 Pa·s<br>Correction factor = 1.1603 | | T = 313.15 K; P =13.7 MPs<br>SC-$CO_2$viscosity =5.610 Pa·s<br>Correction factor =1.1428 | |
|---|---|---|---|
| 0.11 | 0.995 | 0.14 | 1.002 |
| 0.92 | 1.022 | 1.34 | 1.058 |
| 1.77 | 1.106 | 2.08 | 1.082 |
| 2.5 | 1.088 | 2.48 | 1.096 |
| 2.69 | 1.111 | 2.21 | 1.077 |

**Tables 7:** Viscosities of Supercritical Carbon dioxide with Different fractions of Oleic acid mixtures [55].

| T = 333.15 K; P = 15.5 MPs<br>SC-$CO_2$ viscosity = 4.930 Pa·s<br>Correction factor = 1.1485 | |
|---|---|
| 0.17 | 1.007 |
| 0.61 | 1.021 |
| 1.3 | 1.047 |
| 1.96 | 1.067 |
| 2.29 | 1.077 |
| 2.53 | 1.081 |
| 2.89 | 1.094 |
| 3.28 | 1.109 |
| 3.36 | 1.108 |
| 3.57 | 1.121 |
| 4.01 | 1.144 |
| 3.84 | 1.124 |

**Tables 8:** Viscosities of Supercritical Carbon dioxide with Different fractions of Oleic acid mixtures [55].

## An Overview of the Cost of Cheap Soluble Organics

### Cost per Ton

Table 9 shows the price of soluble organics. In addition to waste cooking oil, Zhang, et al. [56] report a price of USD 200 per ton.

| | |
|---|---|
| Crude palm oil | 703 |
| Rapeseed oil | 824 |
| Soyabeen oil | 771 |
| Waste cooking oil | 224 |
| Yellow grease | 412 |

**Table 9:** Price in United Sates Dollars per ton of soluble organics [57].

Table 9 shows that the price of waste cooking oil (or used frying oils) is 2.5–3.0 times cheaper than virgin vegetable oils and this coupled with its huge availability makes it attractive for used on carbon dioxide viscosification. Compared to waste

cooking oil, soluble organics from slaughterhouses are waste and the use of these whether as feed stock for anaerobic digesters [58-60] or as soluble organics represents effective waste management [61].

### Theoretical Models of Solute Containing Carbon Dioxide

Theoretically, the effect of solutes on the viscosity of SC-$CO_2$ has been described using the following equation [62]:

$$\eta_r = 1 + Ac^{1/2} + Bc \quad (1)$$

In which $\eta_r$ is the relative viscosity defined as the viscosity containing solute divided by the viscosity without solute, $c$ is the concentration of solute, and *A* and *B* are constants.

The coefficient, *A,* arises from ion interaction, which for is zero for non-electrolytes; hence Equation (1) reduces to:

$$\eta_r = 1 + Bc \quad (2)$$

The *B* coefficient is related to the size and shape of solutes and its effect on the solvent structure. Generally, negative values result from breaking up of solvent structure and positive values show that the solution is more ordered than the solvent structure. For non-electrolyte, the coefficient *B* has been related to the partial molar volume ($V_m$) of the solute using the Einstein equation as:

$$B = 2.5V_m \quad (3)$$

Equation (2) can now be written as:

$$\eta_r = 1 + 2.5V_m c \quad (4)$$

The implication of Equation (4) is that since there cannot be negative values of concentration or partial molar volume of organic solutes [63] (Table 2), the relative viscosity of SC-$CO_2$ containing soluble organics will be greater than unity. This indicates that the viscosity of SC-$CO_2$ will be increased by soluble organics and this explains the trends as seen in preceding tables.

## Relevance of Carbon Dioxide Viscosity on Interfacial Instability in Two-phase flow Regime

### Interfacial Instability in Fluid Injection into Porous Media

Saffman and Taylor [64] demonstrated theoretically and experimentally that the interface between two immiscible fluids in a porous medium can become unstable if accelerated and the condition of stability will be governed by whether the acceleration is directed from the denser or less dense phase fluid. In this regard, the most important lesson to be learned about immiscible displacement is that when a low viscosity fluid is injected to displace a more viscous fluid, fingering instability occurs [65,66]. Accordingly, viscous instability fingering has been reported in carbon dioxide enhanced oil recovery [67]. When instability develops related to a vertical fluid interface it can be amplified depending on the hydrodynamic conditions of the displacement. In this regard, if instability results in an initial displacement that becomes amplified with time then the ratio of the interfacial disturbance at a time to the initial disturbance is given as [68].

$$\frac{\eta}{\eta_o} = \cosh\sqrt{\left\{\frac{4\pi s}{\lambda}\frac{(g_1 - g)}{g_1}\frac{(\rho_2 - \rho_1)}{(\rho_2 + \rho_1)}\right\}}$$

$$s = \frac{1}{2}g_1 t^2 \quad (5)$$

Where;

$\eta$ = interfacial disturbance at a given time
$\eta_0$ = initial interfacial disturbance
$g_1$ = vertically downward acceleration
$g$ = vertically upward acceleration
$\rho_2$ = density of accelerated fluid
$\rho_1$ = density of accelerating fluid
$\lambda$ = wavelength of the disturbance
$t$ = is time

Equation 5 shows that interfacial instability is directly proportional to density difference and since there is a correlation between density and viscosity; instability must be proportional to the difference in the dynamic viscosity of fluids. The interfacial instability that is characterized by a rich variety of interfacial pattern or morphology is like that observed in a Hele-Shaw cell, but the hydrodynamic stability associated with this system has been difficult to resolve. This is because as the unstable mode of perturbation becomes amplified, they become coupled in a weakly nonlinear stage of evolution and finally evolve into a complicated finger like structure that is dominated by nonlinear effect [69]. However, the pioneering work of Saffman and Taylor [64] motivated subsequent theoretical and experimental study of interfacial instability related to porous media immiscible fluid displacements. The obvious motivation for this is that the porous medium is characterized by a complex domain of varying pore size distribution which enhances interfacial problems. In this regard, Stokes, et al. [70] found

experimentally that some parameters govern interfacial morphologies under viscous instability conditions. The factors are the dynamic viscosity of fluids, flow rate, the surface tension between fluids, the absolute permeability of the porous medium and the ease with which the two fluids wet the porous system. They reported that if the displacing fluid preferentially wets the porous system, then the width of the finger-like instability is larger than the characteristic pore size. Under this condition, the width follows a scaling law that is governed by the interfacial tension, flow rate and the permeability of the porous medium. On the contrary, if the displaced fluid preferentially wets the porous medium then the width of the finger is of the same order as the characteristic pore size and independent of other factors.

In furthering the work of Saffman and Taylor [64], Chuoke, et al. [71] showed that when an initially planner interface between two fluid is displaced by a constant velocity normal to the front, an instability arises when the velocity exceeds a critical velocity. He presented the following theoretical finding:

$$\left(\frac{\mu_2}{k_2}+\frac{\mu_1}{k_1}\right)U_c+(\rho_2-\rho_1)g\cos(zz')=0 \quad (6)$$

Where:

$\mu_1$ = dynamic viscosity of displacing fluid
$\mu_2$ = dynamic viscosity of displaced fluid
$k_1$ = effective permeability of displacing fluid
$k_2$ = effective permeability of displaced fluid
$\rho_1$ = density of displacing fluid

$\rho_2$ = density of displaced fluid

$U_c$ =critical rate

$g$ = gravitational acceleration constant

$\cos(zz')$ = is the direction cosine between the vertical Cartesian coordinate z'(positive upward) and the z coordinate normal to the initially plane macroscopic interface taken positive in the direction from Liquid I to Liquid 2.

When the disturbance occurs, the front will have a wavelength greater than a critical wavelength given as:

$$\lambda_c=2\pi\left[\frac{\sigma^*}{\left(\frac{\mu_2}{k_2}-\frac{\mu_1}{k_1}\right)(U-U_c)}\right]^{3/2} \quad (7)$$

Where:
$U$ = velocity of displacement
$\lambda_c$ = critical wavelength of in stability
$\sigma^*$ = effective interfacial tension which integrates information on wettability

Chuoke's work introduced the concept of a dimensionless group that characterizes a combination of the factors governing interfacial instability. Following his work, several interfacial stability analyses [71-73] have shown that the fundamental factors affecting interfacial instability are mobility or viscosity ratio, displacement velocity, capillary and gravitational forces, permeability and wettability.

Peter and Flock [74] studied interfacial stability of a radial and rectangular system. Their study resulted in the definition of a dimensionless lumped parameter defining a stability index. Based on this stability index, the condition for a stable displacement is given as:

$$\frac{\sigma^*}{r_a^2}\left[\frac{(M-1)(v-v_c)\mu_w r_a^2}{\sigma^* k_{wor}}\right]^{3/2}-(r_a\gamma)>0$$

$$M=\frac{k_{wor}\mu_o}{k_{oiw}\mu_w} \quad (8)$$

Where:

$\gamma$ = wave number $m^{-1}$

$k_{wor}$ = effective permeability of water at residual oil saturation

$k_{oiw}$ = effective permeability of oil at residual water saturation
$v$ = average velocity of flooding
$v_c$ = critical velocity of flooding
$r_a$ = radius of core for the cylindrical system
The following stability number was presented for a cylindrical system

$$I_{SC}=\left(\frac{\mu_o}{\mu_w}-1\right)\frac{v\mu_w}{C^*\sigma k} \quad (9)$$

Where:

$I_{SC}$ = dimensionless stability number for a cylindrical system
$C^*$ = wettability number
$k$ = absolute permeability

## Implication of Viscosity Increase of Supercritical Carbon Dioxide on Geological Sequestration Projects

### Implications for Sweep Efficiency

For multi-phase flow in porous media, the mobility of a fluid is defined as the ratio of its effective permeability to its dynamic viscosity. For water injection for improved oil recovery, a mobility ratio is defined as the ratio of the mobility of the injected gas to the mobility of the displaced oil in the porous medium. For gas injection into a saline aquifer, this parameter is defined as the reciprocal of the ratio given as [74]:

$$M = \frac{k_{wig}\mu_g}{k_{gwr}\mu_w} \quad (10)$$

Where:

$M$ = mobility ratio

$k_{wig}$ = relative permeability of water at irreducible gas saturation

$k_{gwr}$ = relative permeability of gas at residual water saturation

$\mu_w$ = dynamic viscosity of water

$\mu_g$ = dynamic viscosity of gas

In the literature, a favorable mobility ratio is the one where the mobility of the displacing fluid is lower than that of the displaced fluid. Generally, higher mobility ratios are characterized by higher relative permeabilities, permeability heterogeneities and adverse viscosity ratios where the viscosity of the injected fluid is significantly lower than that of the displaced fluid. An interesting correlation between injection sweep efficiency and mobility ratio is seen in Figure 4. Accordingly, lower mobility ratios are required for higher sweep efficiencies for a given fractions flow of the injected fluid.

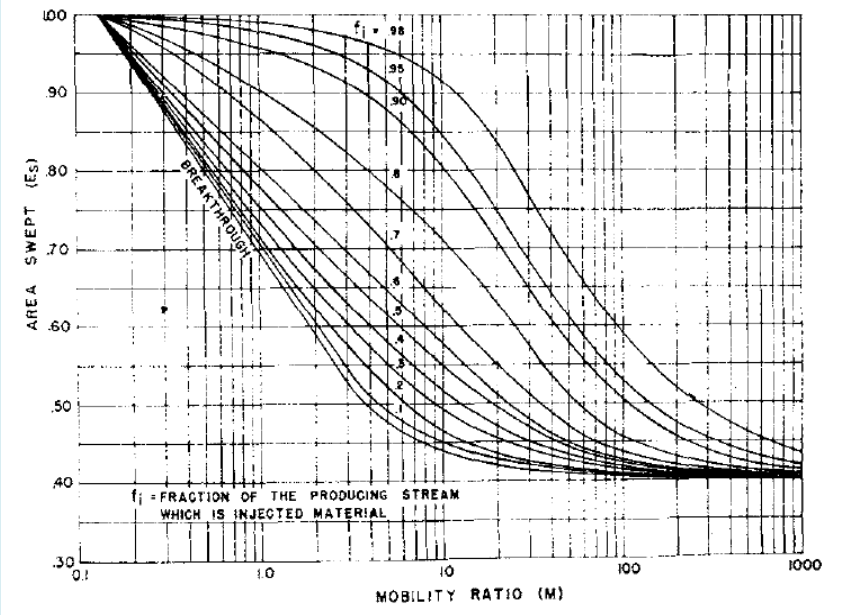


**Figure 4:** Areal sweep efficiency versus mobility ratio as function of injected fluid fractional flow [75].

One major problem associated with fluid injection for improved oil recovery has long been encountered in the petroleum industry [76]. This is the adverse mobility ratio problem that arises when the viscosity of the injected fluid is less than that of the displaced fluid in the porous medium. In carbon dioxide, enhanced oil recovery from petroleum reservoirs, the adverse mobility ratio coupled with heterogeneity has been one of the causes of poor sweep efficiency [77]. To circumvent this problem, carbon dioxide thickeners have been used to increase viscosity [78] and this has led to enhance mobility control in carbon dioxide enhanced oil recovery [79]. Evidence from relative viscosity data of supercritical carbon dioxide containing soluble organics reported in this paper is an indication that the increased viscosity could result in a favorable mobility ratio in carbon dioxide injection into saline aquifers where significant viscosity contrast exists [80]. The increase advantage on mobility ratio can be seen from the above

equation if the viscosity of water, which is the injected fluid, is substituted for the viscosity of injected carbon dioxide. The result is an increase in the denominator of the equation, implying a decrease in mobility ratio.

### Implication for Maximum Gas Saturation

The effect of carbon dioxide viscosity increase on maximum gas saturation can be correlated with the critical velocity equation. Considering the mobility ratio for gas injection as being the reciprocal of that for water injection, the criterion for stability number becomes:

$$\frac{\gamma\sigma^*}{r_a^2}\left[\frac{(M-1)(v-v_c)\mu_g r_a^2}{\sigma^* k_{gwr}}\right]^{3/2} - (r_a\gamma) > 0 \quad (11)$$

From this equation, the critical velocity can be obtained as:

$$v_c = v - \frac{\left[\frac{r_a^3}{\sigma}\right]^{3/2}\sigma^* k_{gwr}}{\left(\frac{k_{wig}}{k_{gwr}}\frac{\mu_g^2}{\mu_w}\right)} \quad (12)$$

By writing flooding velocity in terms of injection rate Equation 12 becomes:

$$v_c = \frac{Q_{inj}}{A_c} - \frac{\left[\frac{r_a^3}{\sigma}\right]^{3/2}\sigma^* k_{gwr}}{\left(\frac{k_{wig}}{k_{gwr}}\frac{\mu_g^2}{\mu_w}\right)} \quad (13)$$

Where:

$Q_{inj}$ = gas injection rate

$A_c$ = cross sectional area of injection

From this equation, increasing injected carbon dioxide dynamic viscosity means increasing the denominator which corresponds to decreasing the last term on the right-hand side of the equation. This will result in a net decrease of this term and a corresponding increase in critical velocity. Consequently, larger flow rates are required to achieve critical velocities, which is an added advantage because above the critical velocity instability occurs with increasing number of fingers leading to fractal interfacial morphology and viscous fingering. This means increasing gas- water viscosity ratio or decreasing water-gas viscosity ratio will result in maximum gas saturation at the end of the injection due to increase stable displacement. Figure 5 represents a plot of water-gas viscosity ratio versus maximum gas saturation. Accordingly, the figure shows that as water-gas viscosity ratio decreases there is an increase in maximum gas saturation as expected from Equation12 of our work.

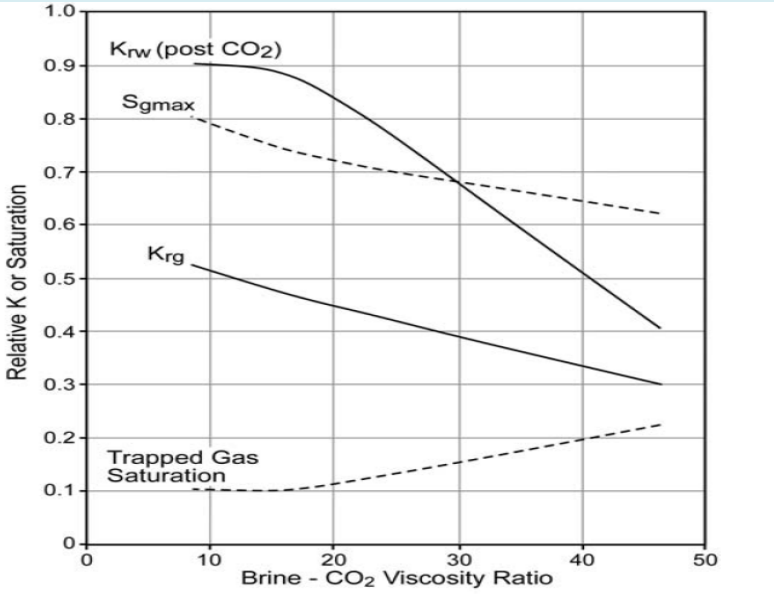


**Figure 5:** Effect of water-carbon dioxide viscosity ratio on maximum gas saturation [81].

### Implication for Critical Velocity from Chuoke Model

The effect of increase dynamic viscosity of carbon dioxide on critical velocity can be realized from the work of Chuoke, et al. [73]. His equation for instability conditions is given as:

$$\left(\frac{\mu_2}{k_2}+\frac{\mu_1}{k_1}\right)U_c+(\rho_2-\rho_1)g\cos(zz')=0 \quad (14)$$

From this equation, the critical velocity for the onset of instability is given as:

$$U_c=\frac{-(\rho_2-\rho_1)g\cos(zz')}{\left(\frac{\mu_2}{k_2}-\frac{\mu_1}{k_1}\right)} \quad (15)$$

This equation written for carbon dioxide injection into a saline aquifer gives:

$$U_c=\frac{(\rho_{CO_2}-\rho_b)g\cos(zz')}{\left(\frac{\mu_b}{k_b}-\frac{\mu_{CO_2}}{k_{CO_2}}\right)} \quad (16)$$

For a given injection scenario, the wettability factor in a saline aquifer will decrease [82]. The presence of soluble organics in supercritical carbon dioxide will increase the density of brine under aquifer temperature and pressure conditions. Gravity is constant at a given location and effective permeabilities will be determined by prevailing wetting conditions. Therefore, increasing the dynamic viscosity of supercritical carbon dioxide corresponds to decreasing the denominator of Equation 15. Increasing the density of this phase also means decreasing the denominator. Therefore, decrease in density difference coupled with decrease in effective interfacial tension due to wettability decrease means an overall decrease in the numerator. The net effect is an increase in critical velocity of flooding since the density difference is negative. The critical velocity of flooding for a given injection scenario is the velocity at which the onset interfacial instability cannot be damped leading to amplification. Therefore, the lower the value of this velocity the greater the chances of instability occurring. One would, therefore, prefer a higher critical velocity because this gives the option to increase injection velocity without any danger of instability growing [83]. Figure 6 illustrates the effect of flooding rate on interface morphology.

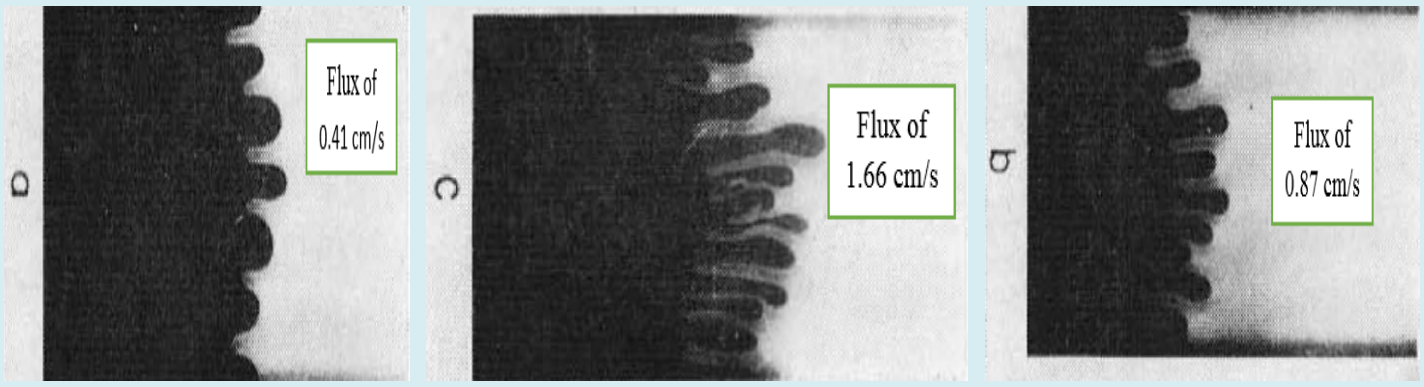


**Figure 6:** Photograph of the interface between injected and displacing fluid for different fluxes [71].

The photos in Figure 6 show that at the onset of instability, increasing flooding velocity or flux results in increasing the number of fingers at the interface. Consequently, at a flux of 0.41 cm/s, the number of fingers is 7. At a flux of 0.87 cm/s, the number of fingers is 9 while at a flux of 1.66 cm/s, the number of fingers is 13. This has the potential to introduce a fractal advance nature which reduces sweep efficiency.

### Implication for Interfacial Stability

Experience from the petroleum industry shows that while unfavorable mobility ratios are some of the principal causes of poor sweep efficiency, interfacial instability characterized by viscous fingering [84] is another cause of poor sweep efficiency. Consequently, to deal with interfacial instability problems in improved oil recovery, linear stability analyses approaches have been employed. The principal objective of such analyses is to first, theoretically and mathematically describe the instability problem and to use this as the basis for predicting the onset of instability. Thus, the theoretical works so far cited in this paper provide fertile grounds for predicting the onset of instability in each carbon dioxide injection project. The reason is that interface instability is the direct result of several factors including viscosity contrast and this is characteristic of carbon dioxide injection into geologic repositories. Therefore, the implication of viscosity increase due to the presence of soluble organics in supercritical carbon dioxide will be discussed in the following contexts:

### Implication for Stability Number

Generally, the condition for instability based on Peters and Flock [74] work is that this dimensionless number must be positive for a given injection scenario. This number is given as:

$$\frac{\gamma\sigma^*}{r_a^2}\left[\frac{(M-1)(v-v_c)\mu_g r_a^2}{\sigma^* k_{gwr}}\right]^{3/2} - (r_a\gamma) > 0 \quad (16)$$

$$M = \frac{k_{wig}}{k_{gwr}}\frac{\mu_g}{\mu_w}$$

To be able to determine the effect of injection fluid dynamic viscosity increase requires rewriting this equation in a more objective manner. This can be done by inserting the definition of mobility *M*, into the definition for stability number criterion. The result gives Equation 11 as before:

$$\frac{\gamma\sigma^*}{r_a^2}\left[\frac{\left(\left(\frac{k_{wig}}{k_{gwr}}\frac{\mu_g^2}{\mu_w}\right)-\mu_g\right)(v-v_c)\mu_g r_a^2}{\sigma^* k_{gwr}}\right]^{3/2} - (r_a\gamma) > 0 \quad (11)$$

For an injection project, the wettability of the system fixes the endpoint effective permeabilities $k_{oiw}, k_{wor}$ of the fluids found in this equation. Also, for given flooding velocity, $v$, the critical velocity $v_c$ for the onset of instability is constant. The wave number and effective interfacial tension are also constant. Consequently, increasing the dynamic viscosity of injected carbon dioxide means increasing the quantity in the numerator. Wettability studies of the system, carbon dioxide-brine-solid so far has shown that the wettability of the system will decrease with carbon dioxide injection [82]. This means the effective interfacial tension in the denominator will decrease. The net effect has the potential to increase the left-hand side of the equation and will result in higher values of the stability number for a given geometry. Theoretically, this corresponds to increasing flooding velocities with less chances of attaining critical velocities.

### Effect of Critical Velocity Increase on Equilibrium Saturation of Injected Carbon Dioxide

In geological carbon storage, the equilibrium saturation defined as injected gas saturation that is free gas in the formation at the end of injection is of interest because it correlates with the volume of subsurface pore space that has been effectively unitized [85]. Generally, low capillary number injections are responsible for viscous fingering which reduces the equilibrium saturation. Figure 7 shows a plot of free gas saturation versus the logarithm of the capillary number.

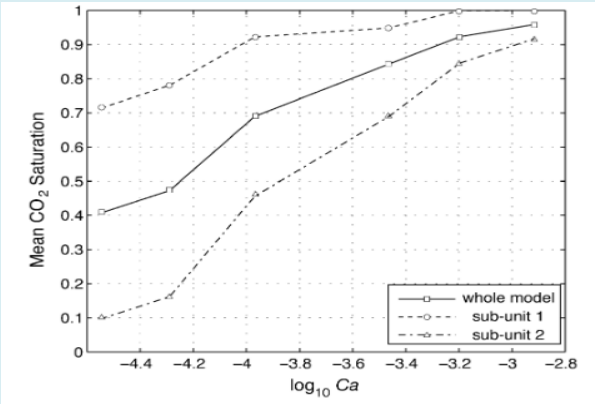


**Figure 7:** Equilibrium gas saturation versus the logarithm of capillary number [86].

The figure shows that higher capillary numbers favor higher free gas saturation for a given injection scenario. Higher capillary number here correlates with increase injection gas velocity or increase velocity of injection or both.

### Implication for the Critical Wavelengths of the Instability

Choke, et al. [87] critical wavelength is calculated using Equation 7 as:

$$\lambda_c = 2\pi\left[\frac{\sigma^*}{\left(\frac{\mu_2}{k_2}-\frac{\mu_1}{k_1}\right)(U-U_c)}\right]^{3/2} \quad (7)$$

The viscosity has a qualitative effect on the wavelength at the onset of instability such that the wavelength increases for higher viscosities of the injected fluid [88]. The effect of increased dynamic viscosity $\mu_1$ of injected carbon dioxide is to reduce the quantity related to viscosity in the bracket found in the denominator. The net effect will be an increase in the wavelength of the critical instability.

## Summary and Conclusion

Global warming due to unprecedented emission of anthropogenic greenhouse gases is the major environmental challenge in the 21st Century. Among the greenhouse gases, anthropogenic carbon dioxide has the greatest presence in the atmosphere and the most notable greenhouse gas regarding the gaseous radiative forcing effect on climate warming. To reduce climate warming, geological sequestration of anthropogenic carbon dioxide has been accepted as a technically and economically viable option. However, in view of the rate of current emissions from sources as well as possible trends in projected emissions during this century, efficient geological sequestration is necessary to meet reduction targets set by the Intergovernmental Panel on Climate Change (IPCC).

Technically, efficient geological storage of anthropogenic carbon dioxide is linked to efficient displacing of formation brine. Inherent in the displacement process is the interfacial instability due to the sharp contrast between the dynamic viscosity of carbon dioxide and formation brine. In the petroleum industry, enhanced oil recovery using carbon dioxide depends on using costly polymers for carbon dioxide thickening. However, due to the emphasis on the supercritical state of carbon dioxide geological sequestration, the solubility potential of cheap or waste soluble organics can be a means of increasing the dynamic viscosity that can reduce the interfacial instability problem. In this paper, we have reviewed literature to bring to the attention of the geological sequestration community some important facts about the availability of cheap soluble organics and their potential in increasing supercritical carbon dioxide viscosity. We have also discussed the effect of dynamic viscosity increase on interfacial stability. The following sums up our conclusion of this paper:

1. There exists a huge potential for using cheap soluble organics for increasing the dynamic viscosity of carbon dioxide
2. Among the cheap soluble organics, waste cooking oil which has a sustained promising global abundance due to the growth trends in world population
3. Increasing dynamic viscosity of carbon dioxide using soluble organics will increase the critical velocity of injection required for the onset of interfacial instability. The advantage is that it offers the opportunity to inject carbon dioxide at higher rates without exceeding the critical velocity.
4. Increase injection velocity without the risk of exceeding the critical velocity means increased capillary number which could undermined capillary forces and increase displacement efficiency of formation brine leading to maximization of carbon dioxide geological storage

## Acknowledgements

We wish to acknowledge the timely contributions to our work by the document delivery section of the Library, and the Office of Research and Graduate Studies, Cape Breton University. They have made it possible to complete this manuscript on time.

## Nomenclature

| |
|---|
| $\eta_r$ is the relative viscosity-cp |
| $c$ is the concentration of solute |
| $A$ and $B$ are constants of Equation 1. |
| $V_m$ is molar volume |
| s is distance |
| $\eta$ is interfacial disturbance at a given time |
| $\eta_0$ is initial interfacial disturbance |
| $g_1$ is vertically downward acceleration |
| $g$ is vertically upward acceleration |
| $\rho_2$ is density of accelerated fluid |

| |
|---|
| $\rho_1$ is density of accelerating fluid |
| $\lambda$ is wavelength of the disturbance |
| $t$ is is time |
| $\mu_1$ is dynamic viscosity of displacing fluid |
| $\mu_2$ is dynamic viscosity of displaced fluid |
| $k_1$ is effective permeability of displacing fluid |
| $k_2$ is effective permeability of displaced fluid |
| $\rho_1$ is density of displacing fluid |
| $\rho_2$ is density of displaced fluid |
| $U_c$ is critical rate |
| $g$ is gravitational acceleration constant |
| $\cos(zz')$= is the direction cosine between the vertical Cartesian coordinate z'(positive upward) and the z coordinate normal to the initially plane macroscopic interface taken positive in the direction from Liquid 1 to Liquid 2. |
| $U$ is velocity of displacement |
| $\lambda_c$ is critical wavelength of in stability |
| $\sigma^*$ =iseffective interfacial tension which integrates information on wettability |
| M is relative mobility ratio |
| $\gamma$ is wave number |
| $k_{wor}$ is effective permeability of water at residual oil saturation |
| $k_{oiw}$ is effective permeability of oil at residual water saturation |
| $v$ is average velocity of flooding |
| $v_c$ is critical velocity of flooding |
| $r_a$ is radius of core for the cylindrical system |

| |
|---|
| $I_{SC}$ is dimensionless stability number for a cylindrical system |
| $C^*$ is wettability number |
| $k$ is absolute permeability |
| $k_{wig}$ is relative permeability of water at irreducible gas saturation |
| $k_{gwr}$ is relative permeability of gas at residual water saturation |
| $\mu_w$`is dynamic viscosity of water |
| $\mu_g$ is dynamic viscosity of gas |
| $Q_{inj}$ is gas injection rate |
| $A_c$ is cross sectional area of injection |

## References

1. Dyurgerov MB, Meier MF (2000) Twentieth century climate change: Evidence from small glaciers. Proc Natl Acad Sci USA 97(4): 1406-1411.

2. Croiset E, Thambimuthu KV (2001) NOx and $SO_2$ emissions from $O_2/CO_2$ recycle coal combustion. Fuel 80(14): 2117-2121.

3. Bruce JP, Lee H, Haites EF (1996) Climate Change 1995-Economic and Social Dimensions of Climate Change, Cambrifge University Press, pp: 458.

4. Meadows DH, Meadows DL, Randers J (1993) Beyond the Limits: An Executive Summary. Bull Sci Tech Soc 13: 3-14.

5. Canadell JG, Quéré CL, Raupach MR, Field CB, Buitenhuis ET, et al. (2007) Contributions to accelerating atmospheric $CO_2$ growth from economic activity, carbon intensity, and efficiency of natural sinks. Proc Natl Acad Sci USA 104(47): 18866-18870.

6. Raupach MR, Marland G, Ciais P, Quéré CL, Canadell JG, et al. (2007) Global and regional drivers of accelerating CO2 emissions. Proc Natl Acad Sci USA 104(24): 10288-10293.

7. Oberthür S, Ott HE (1999) The Kyoto Protocol: international climate policy for the 21st century. Springer,

Berlin, Heidelberg.

8. Bodansky D (2010) The Copenhagen climate change conference: a postmortem American Journal of International Law 104(2): 230-240.

9. Myhre G, Highwood EJ, Shine KP, Stordal F (1998) New estimates of radiative forcing due to well mixed greenhouse gases. Geophysical Research Letters 25(14): 2715-2718.

10. Olah GA, Goeppert A, Prakash GKS (2009) Chemical recycling of carbon dioxide to methanol and dimethyl ether: from greenhouse gas to renewable, environmentally carbon neutral fuels and synthetic hydrocarbons. J Org Chem 74(2): 487-498.

11. Bachu S (2000) Sequestration of $CO_2$ in geological media: criteria and approach for site selection in response to climate change. Energy conversion and Management 41(9): 953-970.

12. Sabine CL, Feely RA, Gruber N, Key RM, Lee K, et al. (2004) The oceanic sink for anthropogenic $CO_2$. Science 305(5682): 367-371.

13. Mayfield KJ, Shalliker RA, Catchpoole HJ, Sweeney AP, Wong V, et al. (2005) Viscous fingering induced flow instability in multidimensional liquid chromatography. J Chromatogr A 1080(2): 124-131.

14. Hyatt JA (1984) Liquid and supercritical carbon dioxide as organic solvents. J Org Chem 49(26): 5097-5101.

15. Battimelli A, Carrère H, Delgenès JP (2009) Saponification of fatty slaughterhouse wastes for enhancing anaerobic biodegradability. Bioresource Technology 100(15): 3695-3700.

16. Nollet LM, Toldrá F (2006) Advanced technologies for meat processing CRC Press, pp: 483.

17. Nordbotten JM, Celia MA, Bachu S (2005) Injection and storage of $CO_2$ in deep saline aquifers: Analytical solution for $CO_2$ plume evolution during injection. Transport in Porous media 58(3): 339-360.

18. Pruess K, Garcia J (2002) Multiphase flow dynamics during $CO_2$ disposal into saline aquifer. Environmental Geology 42(2-3): 282-295.

19. Homsy GM (1987) Viscous fingering in porous media. Annual review of fluid mechanics 19(1): 271-311.

20. Campbell BT, Orr FM (1985) Flow visualization for CO2/crude-oil displacements. Society of Petroleum Engineers Journal 25(5): 665-678.

21. Riaz A, Hesse M, Tchelepi HA, Orr FM (2006) Onset of convection in a gravitationally unstable diffusive boundary layer in porous media. Journal of Fluid Mechanics 548(1): 87-111.

22. Gislason SR, Wolff Boenisch D, Stefansson A, Oelkers EH, Gunnlaugsson E, et al. (2010) Mineral sequestration of carbon dioxide in basalt: A pre-injection overview of the CarbFix project. International Journal of Greenhouse Gas Control 4(3): 537-545.

23. Brigham WE, Reed PW, Dew JN (1961) Experiments on mixing during miscible displacement in porous media. Society of Petroleum Engineers Journal 1(10): 1-8.

24. Van Engelenber B, Blok K (1992) Prospects for the Disposal of Carbon Dioxide in Aquifers. University of Report No. G-91006. Department of Science Technology and Society. Utrecht, The Netherland.

25. Kovscek AR, Cakici MD (2005) Geologic storage of carbon dioxide and enhanced oil recovery. II. Cooptimization of storage and recovery. Energy Conversion and Management 46(11): 1941-1956.

26. Shi C, Huang Z, Beckman EJ, Enick RM, Kim SY, et al. (2001) Semi-fluorinated trialkyltin fluorides and fluorinated telechelic ionomers as viscosity-enhancing agents for carbon dioxide. Industrial & engineering chemistry research 40( 3): 908-913.

27. Enick RM, Ammer J (1998) A literature review of attempts to increase the viscosity of dense carbon dioxide pp:1-48.

28. Xu J (2003) Carbon dioxide thickening agents for reduced CO2 mobility. Doctoral dissertation, University of Pittsburgh.

29. Heller JP, Dandge DK, CardRJ, Donaruma LG (1985) Direct thickeners for mobility control of CO2 floods. Society of Petroleum Engineers Journal 25(5): 679-686.

30. Yazdi AV, Beckman EJ (1995) Design of highly CO2-soluble chelating agents for carbon dioxide extraction of heavy metals. Journal of materials research 10(3): 530-537.

31. Luo W (2012) Coupling of Hydrocarbon Solvents of Hot Water for Enhanced Heavy Oil Recovery . Doctoral dissertation, Faculty of Graduate Studies and Research, University of Regina, Regina. PP: 1-32.

32. Enick RM, Beckman EJHZH, Xu JH, Kilic S, Shi C (2000) Improved geologic sequestration using carbon dioxide thickeners. Abstract of Papers of the American Chemical Soceity, pp: 398-398.

33. van Larebeke N, Hens L, Schepens P, Covaci A, Baeyens J, et al. (2001) The Belgian PCB and dioxin incident of January-June 1999: exposure data and potential impact on health. Environmental Health Perspectives 109(3): 265-273.

34. Kale MC, Aral Y, Aydın E, Cevger Y, Sakarya E, et al. (2011) Determination of by-product economic values for slaughtered cattle and sheep. Kafkas Universitesi Veteriner Fakultesi Dergisi 17(4): 551-556.

35. Arvanitoyannis IS , Kassaveti A (2008) Fish industry waste: treatments, environmental impacts, current and potential uses. International Journal of Food Science & Technology 43(4): 726-745.

36. Masters E, Yidana J, Lovett P (2005) Reinforcing sound management through trade: shea tree products in Africa.

37. Nelson L, Seager J (2008) A companion to feminist geograph. John Wiley & Sons.

38. Chalfin B (2004) Shea butter republic. State power, global markets, and the making of an indigenous commodity, Psychology Press.

39. Elias M, Carney J (2007) African shea butter: A feminized subsidy from nature, Africa 77: 37-62.

40. Kulkarni MG, Dalai AK (2006) Waste cooking oil an economical source for biodiesel: a review. Industrial & engineering chemistry research 45(9): 2901-2913.

41. Wiltsee G (1998) Waste grease resource in 30 US metropolitan areas. Proceedings of Bioenergy 98 Conference, Wisconsin.

42. Chhetri AB, WattsKC, Islam MR (2008) Waste cooking oil as an alternate feedstock for biodiesel production. Energies 1(1): 3-18.

43. Yaakob Z, Mohammad M, Alherbawi M, Alam Z, Sopian K (2013) Overview of the production of biodiesel from waste cooking oil. Renewable and sustainable energy reviews 18: 184-193.

44. Radich A (2006) US Energy Information Administration.

45. Canada S (2006) Statistics Canada, Demography Division.

46. Carter D, Darby D, Halle J, Hunt P (2005) How to Make Biodiesel; Low-Impact Living Initiative, Redfield Community, Winslow, Bucks.

47. Froning GW, Wehling RL, Cuppett SL, Pierce MM, Niemann L, et al. (1990) Extraction of cholesterol and other lipids from dried egg yolk using supercritical carbon dioxide. Journal of Food Science 55(1): 95-98.

48. Reverchon E (1997) Supercritical fluid extraction and fractionation of essential oils and related products. The Journal of Supercritical Fluids 10(1): 1-37.

49. Dhellot JR, Matouba E, Maloumbi MG, Nzikou JM, Ngoma DS, et al. (2006) Extraction, chemical composition and nutrional characterization of vegetable oils: Case of Amaranthus hybridus (var 1 and 2) of Congo Brazzaville. African Journal of Biotechnology 5(11).

50. Vaquero EM, Beltrán S, Sanz MT (2006) Extraction of fat from pigskin with supercritical carbon dioxide. The Journal of supercritical fluids 37(2): 142-150.

51. Marsal A, Celma PJ, Cot J, Cequier M (2000) Supercritical CO2 extraction as a clean degreasing process in the leather industry. The Journal of Supercritical Fluids 16(3): 217-223.

52. Meng X, Chen G Wang Y (2008) Biodiesel production from waste cooking oil via alkali catalyst and its engine test. Fuel Processing Technology 89(9): 851-857.

53. Hong SA, Kim J, Kim JD, Kang JW, Lee YW (2010) Purification of waste cooking oils via supercritical carbon dioxide extraction. Separation Science and Technology 45(8): 1139-1146.

54. Rincon J, Camarillo R, Rodriguez L, Ancillo V (2010) Fractionation of used frying oil by supercritical CO2 and cosolvents. Industrial & Engineering Chemistry Research 49(5): 2410-2418.

55. Yener ME, Kashulines P, Rizvi SS, Harriott P (1998) Viscosity measurement and modeling of lipid-supercritical carbon dioxide mixtures. The Journal of Supercritical Fluids 11(3): 151-162.

56. Zhang Y, Dube MA, McLean DD, Kates M (2003) Biodiesel production from waste cooking oil: 2. Economic assessment and sensitivity analysis. Bioresource technology 90(3): 229-240.

57. Demirbas A (2008) Economic and environmental impacts of the liquid biofuels. Energy Educat Sci Technol 22: 37-58.

58. Sayed S, de Zeeuw W, Lettinga G (1984) Anaerobic treatment of slaughterhouse waste using a flocculant sludge UASB reactor. Agricultural wastes 11(3): 197-226.

59. Mshandete A, Kivaisi A, Rubindamayugi M, Mattiasson B (2004) Anaerobic batch co-digestion of sisal pulp and fish wastes. Bioresource technology 95(1): 19-24.

60. Gómez X, Otero M, Morán A (2008) Anaerobic digestion of solid slaughterhouse waste (SHW) at laboratory scale: influence of co-digestion with the organic fraction of municipal solid waste (OFMSW). Biochemical Engineering Journal 40(1): 99-106.

61. Johns MR (1995) Developments in wastewater treatment in the meat processing industry: A review. Bioresource technology 54(3): 203-216.

62. Andrew PA, Hope EG, Palmer DJ (2007) Effect of solutes on the viscosity of supercritical solutions. The Journal of Physical Chemistry B 111(28): 8114-8118.

63. Maham Y, Teng TT, Hepler LG, Mather AE (1994) Densities, excess molar volumes, and partial molar volumes for binary mixtures of water with monoethanolamine, diethanolamine, and triethanolamine from 25 to 80 C. Journal of solution chemistry 23: 195-205.

64. Saffman PG, Taylor G (1958) The penetration of a fluid into a porous medium or Hele-Shaw cell containing a more viscous liquid. Proceedings of the Royal Society of London A: Mathematical, Physical and Engineering Sciences 245(1242).

65. Juanes R, Blunt MJ (2006) Analytical solutions to multiphase first-contact miscible models with viscous fingering. Transport in Porous Media 64(3): 339-373.

66. Onishi K, Matsuoka T, Ishikawa Y, Okamoto I, Xue Z (2009) Measuring Electrical Resistivity Variations in a Sandstone Specimen Injected with Gas, Liquid, and Supercritical $CO_2$. In: Grobe M, Pashin JC (Eds.), Carbon dioxide sequestration in geological medi. State of the science, AAPG Studies in Geology 59(1): 609-618.

67. Boait F, Gandomi J, Johnson G (2015) Enhanced Oil Recovery and Carbon Dioxide Storage. SCCS. Measurement, Monitoring and Verification.

68. Taylor G (1950) The instability of liquid surfaces when accelerated in a direction perpendicular to their planes. Proceedings of the Royal Society A 201(1065).

69. Miranda J, Widom M (1998) Radial fingering in a Hele-Shaw cell: a weakly nonlinear analysis. Physica D: Nonlinear Phenomena 120(3): 315-328.

70. Stokes JP, Weitz DA, Gollub JP, Dougherty A, Robbins MO, et al. (1986) Interfacial stability of immiscible displacement in a porous medium. Physical review letters 57(14): 1718-1721.

71. Chuoke RL, Van Meurs P, Poel vd (1959) The instability of slow, immiscible, viscous liquid-liquid displacements in permeable media. One petro 216(1): 188-194.

72. Van Meurs P (1956) The use of transparent three-dimensional models for studying the mechanism of flow processes in oil reservoirs. Trans 210(1): 295-301.

73. Van Meurs P, Van der Poel C (1958) A theoretical description of water-drive processes involving viscous fingering, Trans AIME 213(1): 103-112.

74. Peters EJ, Flock DL (1981) The onset of instability during two-phase immiscible displacement in porous media. Society of Petroleum Engineers Journal 21(2): 249-258.

75. Caudle BH, Witte (1959) Production potential changes during sweep-out in a five-spot system. Journal of Petroleum Technology 12(12): 63-65.

76. Grogan AT, Pinczewski WV (1987) The role of molecular diffusion processes in tertiary $CO_2$ flooding. Journal of petroleum technology 39(5): 591-602.

77. Jessen K, Kovscek AR, Orr FM (2005) Increasing $CO_2$ storage in oil recovery. Energy Conversion and Management 46(2): 293-311.

78. DeSimone JM, Keiper JS (2001) Surfactants and self-assembly in carbon dioxide. Current opinion in solid state and materials science 5(4): 333-341.

79. Heller JP, Dandge DK, Card RJ, Donaruma LG (1985) Direct thickeners for mobility control of $CO_2$ floods. SPE J 25(5): 679-686.

80. Nordbotten JM, Celia MA, Bachu S (2005) Injection and storage of $CO_2$ in deep saline aquifers: Analytical solution for $CO_2$ plume evolution during injection. Transport in Porous media 58(3): 339-360.

81. Bennion DB, Bachu S (2006) Dependence on temperature, pressure, and salinity of the IFT and relative permeability displacement characteristics of $CO_2$ injected in deep saline aquifers. SPE Annual Technical Conference and Exhibition, USA.

82. Yongman K, Jiamin W, Timothy JK, Tetsu KT (2012) Dewetting of silica surfaces upon reactions with supercritical $CO_2$ and brine: pore-scale studies in micromodels. Environmental science & technology 46(7): 4228-4235.

83. Nittmann J, Daccord G, Stanley HE (1985) Fractal growth of viscous fingers: quantitative characterization of a fluid instability phenomenon. Nature 314(6007): 141-144.

84. Tchelepi HA, Orr FM (1994) Interaction of viscous fingering, permeability heterogeneity, and gravity segregation in three dimensions. SPE Res Eng 9(4): 266-271.

85. Zhang C, Oostrom M, Wietsma TW, Grate JW, Warner MG, et al. (2011) Influence of viscous and capillary forces on immiscible fluid displacement: Pore-scale experimental study in a water-wet micromodel demonstrating viscous and capillary fingering. Energy and Fuels 25(8): 3493-3505.

86. Yamabe H, Tsuji T, Liang Y, Matsuoka T (2014) Lattice Boltzmann Simulations of Supercritical $CO_2$–Water Drainage Displacement in Porous Media: $CO_2$ Saturation and Displacement Mechanism. Environ sci technol 49(1): 537-543.

87. Chuoke RL, van Meurs P, van der Poel C (1959) The instability of slow, immiscible, viscous liquid-liquid displacements in permeable media. One petro 216(1): 199-194.

88. Kumar K, Tuckerman LS (1994) Parametric instability of the interface between two fluids. Journal of Fluid Mechanics 279: 49-68.